J Stat Phys (2011) 142: 657–685
DOI 10.1007/s10955-011-0138-6

# Mean First-Passage Time of Surface-Mediated Diffusion in Spherical Domains

**O. Bénichou · D.S. Grebenkov · P.E. Levitz · C. Loverdo · R. Voituriez**

Received: 16 December 2010 / Accepted: 20 January 2011 / Published online: 2 February 2011


**Abstract** We present an exact calculation of the mean first-passage time to a target on the surface of a 2D or 3D spherical domain, for a molecule alternating phases of surface diffusion on the domain boundary and phases of bulk diffusion. The presented approach is based on an integral equation which can be solved analytically. Numerically validated approximation schemes, which provide more tractable expressions of the mean first-passage time are also proposed. In the framework of this minimal model of surface-mediated reactions, we show analytically that the mean reaction time can be minimized as a function of the desorption rate from the surface.

**Keywords** Random walks · First-passage time · Intermittent search strategies

## 1 Introduction

The kinetics of many chemical reactions is influenced by the transport properties of the reactants that they involve [1, 2]. In fact, schematically, any chemical reaction requires first that a given reactant A meets a second reactant B. This first reaction step can be rephrased as a search process involving a searcher A looking for a target B. In a very dilute regime, exemplified by biochemical reactions in cells [3] which sometimes involve only a few copies of reactants, the targets B are sparse and therefore hard to find in this search process language.

O. Bénichou (✉) · C. Loverdo · R. Voituriez
Laboratoire de Physique Théorique de la Matière Condensée (UMR 7600), case courrier 121, Université Paris 6, 4 Place Jussieu, 75255 Paris Cedex, France
e-mail: benichou@lptl.jussieu.fr

D.S. Grebenkov · P.E. Levitz
Laboratoire de Physique de la Matière Condensée (UMR7643), CNRS – Ecole Polytechnique, 91128 Palaiseau Cedex, France

D.S. Grebenkov
Laboratoire Poncelet (UMI 2615), CNRS – Independent University of Moscow, Bolshoy Vlasyevskiy Pereulok 11, 119002 Moscow, Russia

In such reactions, the first step of search for reactants B is therefore a limiting factor of the global reaction kinetics. In the general aim of enhancing the reactivity of chemical systems, it is therefore needed to optimize the efficiency of this first step of search.

Recently, it has been shown that intermittent processes, combining slow diffusion phases with a faster transport, can significantly increase reactions rates [4–6]. A minimal model demonstrating the efficiency of this type of search, introduced to account for the fast search of target sequences on DNA by proteins [7] is as follows (see also [8–11]). The pathway followed by the protein, considered as a point-like particle, is a succession of 1D diffusions along the DNA strand (called sliding phases) with diffusion coefficient $D_1$ and 3D excursions in the surrounding solution. The time spent by the protein on DNA during each sliding phase is assumed to follow an exponential law with dissociation rate $\lambda$. In this minimal model, the 3D excursions are uncorrelated in space, which means that after dissociation from DNA, the protein will rebind the DNA at a random position independently of its starting position. Assuming further that the mean duration of such 3D excursions $\tau_2$ is finite, it has been shown that the mean first-passage time at the target can be minimized as a function of $\tau_1 = \lambda^{-1}$, as soon as the mean time spent in bulk excursions is not too long. Quantitatively, this condition writes in orders of magnitude as $\tau_2 \leq L^2/D_1$, and the minimum of the search time is obtained for $\tau_1 \simeq \tau_2$ in the large $L$ limit. Note that in this minimal model, where the time $\tau_2$ is supposed to be a fixed exterior parameter, bulk phases are always beneficial in the large $L$ limit (i.e. allow one to decrease the search time with respect to the situation corresponding to 1D diffusion only).

In many practical situations however, the duration of the fast bulk excursions strongly depends on the geometrical properties of the system [12–16] and cannot be treated as an independent variable as assumed in the mean-field (MF) model introduced above. An important generic situation concerns the case of confined systems [17–19], involving transport of reactive molecules both in the bulk of a confining domain and on its boundary, referred to as surface-mediated diffusion in what follows. This type of problems is met in situations as varied as heterogeneous catalysis [20, 21], or reactions in porous media and in vesicular systems [17, 18, 22]. In all these examples, the duration of bulk excursions is controlled by the return statistics of the molecule to the confining surface, which crucially depends on the volume of the system. This naturally induces strong correlations between the starting and ending points of bulk excursions, and makes the above MF assumption of uncorrelated excursions largely inapplicable in these examples.

At the theoretical level, the question of determining mean first-passage times in confinement has attracted a lot of attention in recent years for discrete random walks [23–29] and continuous processes [30–34]. More precisely, the surface-mediated diffusion problem considered here generalizes the so-called narrow escape problem, which refers to the time needed for a simple Brownian motion in absence of surface diffusion to escape through a small window of an otherwise reflecting domain. This problem has been investigated both in the mathematical [22, 35–37] and physical [38–41] literature, partly due to the challenge of taking into account mixed boundary conditions. The case of surface-mediated diffusion brings the additional question of minimizing the search time with respect to the time spent in adsorption, in the same spirit as done for intermittent processes introduced above. The answer to this question is a priori not clear, since the mean time spent in bulk excursions diverges for large confining domains, so that the condition of minimization mentioned previously cannot be taken as granted, even in the large system limit. In this context, first results have been obtained in [42] where, surprisingly enough, it has been found that, even for bulk and surface diffusion coefficients of the same order of magnitude, the reaction time can be minimized, whereas MF treatments (see for instance [39]) predict a monotonic behavior.

**Fig. 1** Model

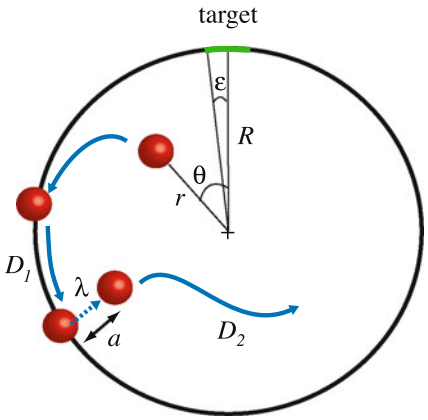


Here, we extend the perturbative results of [42] obtained in the small target size limit. Relying on an integral equation approach, we provide an exact solution for the mean FPT, both for 2D an 3D spherical domains, and for any spherical target size. We also develop approximation schemes, numerically validated, that provide more tractable expressions of the mean FPT.

## 2 The Model

The surface-mediated process under study is defined as follows. We consider a molecule diffusing in a spherical confining domain of radius $R$ (see Fig. 1), alternating phases of boundary diffusion (with diffusion coefficient $D_1$) and phases of bulk diffusion (with diffusion coefficient $D_2$). The time spent during each one-dimensional phase is assumed to follow an exponential law with dissociation rate $\lambda$. At each desorption event, the molecule is assumed to be ejected at a distance $a$ from the frontier (otherwise it is instantaneously readsorbed). Although formulated for any value of this parameter $a$ smaller than $R$, in most physical situations of real interest $a \ll R$. The target is perfectly absorbing and defined in $2D$ by the arc $\theta \in [-\epsilon, \epsilon]$, and in $3D$ by the region of the sphere such that $\theta \in [0, \epsilon]$ where $\theta$ is in this case the elevation angle in standard spherical coordinates. Note that as soon as $\epsilon \neq 0$, the target can be reached either by surface or bulk diffusion. In what follows we calculate the mean first-passage time at the target for an arbitrary initial condition of the molecule.

## 3 2D case

In this section, the confining domain is a disk of radius $R$ and the target is defined by the arc $\theta \in [-\epsilon, \epsilon]$.

### 3.1 Basic Equations

For the process defined above, the mean first-passage time (MFPT) at the target satisfies the following backward equations

$$\frac{D_1}{R^2} t_1''(\theta) + \lambda[t_2(R-a,\theta) - t_1(\theta)] = -1 \quad \text{for } \theta \in [\epsilon, 2\pi - \epsilon], \tag{1}$$

$$D_2\left(\frac{\partial^2}{\partial r^2}+\frac{1}{r}\frac{\partial}{\partial r}+\frac{1}{r^2}\frac{\partial^2}{\partial\theta^2}\right)t_2(r,\theta)=-1, \tag{2}$$

where $t_1$ stands for the MFPT starting from the circle at a position defined on the circumference by the angle $\theta$, and $t_2$ for the MFPT starting from the point $(r,\theta)$ within the disk. In these two equations, the first term of the l.h.s. accounts for the diffusion respectively on the circumference and in the bulk, while the second term of (1) describes desorption events. They have to be completed by two boundary conditions

$$t_2(R,\theta)=t_1(\theta), \tag{3}$$

$$t_1(\theta)=0 \quad \text{for } \theta\in[0,\epsilon]\cup[2\pi-\epsilon,2\pi], \tag{4}$$

which describe the adsorption events and the absorbing target respectively. Equation (2) is easily shown to be satisfied by the following Fourier series

$$t_2(r,\theta)=\alpha_0-\frac{r^2}{4D_2}+\sum_{n=1}^{\infty}\alpha_n r^n\cos(n\theta), \tag{5}$$

with unknown coefficients $\alpha_n$ to be determined. In particular, we aim at determining the search time $\langle t_1\rangle$, defined as the MFPT, with an initial position uniformly distributed on the boundary of the confining domain. Taking (5) at $r=R$, we have

$$\alpha_0-\frac{R^2}{4D_2}+\sum_{n=1}^{\infty}\alpha_n R^n\cos(n\theta)=\begin{cases}t_1(\theta) & \text{if } \theta\in[\epsilon,2\pi-\epsilon],\\ 0 & \text{if } \theta\in[0,\epsilon]\cup[2\pi-\epsilon,2\pi],\end{cases} \tag{6}$$

so that

$$\begin{aligned}\alpha_0-\frac{R^2}{4D_2}&=\frac{1}{2\pi}\int_{\epsilon}^{2\pi-\epsilon}t_1(\theta)\,\mathrm{d}\theta\equiv\langle t_1\rangle,\\ R^n\alpha_n&=\frac{1}{\pi}\int_{\epsilon}^{2\pi-\epsilon}t_1(\theta)\cos(n\theta)\,\mathrm{d}\theta\quad(n\geq 1).\end{aligned} \tag{7}$$

In what follows we will make use of the following quantities:

$$\omega\equiv R\sqrt{\lambda/D_1}, \tag{8}$$

$$x\equiv 1-\frac{a}{R}, \tag{9}$$

and

$$T\equiv\frac{1}{\lambda}+\frac{R^2-(R-a)^2}{4D_2}. \tag{10}$$

As we proceed to show, two different approaches can be used to solve this problem. (i) The first approach, whose main results have been published in [42], uses the explicit form of the Green function for the two-dimensional problem and relies on a small target size $\epsilon$ expansion. We recall these perturbative results below for the sake of self-consistency and give details of the derivation in Appendix A. (ii) The second approach presented next relies on an integral equation which can be derived for $t_1$, and leads to an exact non-perturbative solution.

### 3.2 Perturbative Approach

It is shown in Appendix A that the Fourier coefficients of $t_2(r,\theta)$ as defined in (5) satisfy an infinite hierarchy of linear equations, which lead to the following small $\epsilon$ expansion:

$$\begin{aligned}\alpha_0 &= \frac{R^2}{4D_2} + \omega^2 T\left\{\left(2\sum_{m=1}^{\infty}\frac{1}{\omega^2(1-x^m)+m^2}\right)\right.\\ &\quad\left. -\pi\epsilon + \left(1+2\omega^2\sum_{m=1}^{\infty}\frac{1-x^m}{\omega^2(1-x^m)+m^2}\right)\epsilon^2\right\}+\cdots,\\ \alpha_n &= \frac{\omega^2 T}{R^n(\omega^2(1-x^n)+n^2)}\left\{-2+n^2\epsilon^2+\cdots\right\}.\end{aligned} \tag{11}$$

Note that (11) gives in particular the first terms of the perturbative expansion of the search time $\langle t_1\rangle$ defined in (7) and given in [42]. It should be stressed that since the coefficients of $\epsilon^k$ of this expansion diverge with $\omega$, in practice one finds that the range of applicability in $\epsilon$ of this expansion is wider for $\omega$ small.

### 3.3 Integral Equation for $t_1$

In this section, we first show that the resolution of the coupled PDEs (1), (2) amounts to solving an integral equation for $t_1$ only. As we proceed to show, this integral equation can be solved exactly. Writing (1) as

$$\frac{\partial^2 t_1}{\partial\theta^2} = -\frac{R^2}{D_1} - \omega^2[t_2(R-a,\theta) - t_2(R,\theta)], \tag{12}$$

and expanding its right-hand side into a Taylor series leads to

$$\frac{\partial^2 t_1}{\partial\theta^2} = -\frac{R^2}{D_1} - \omega^2\sum_{k=1}^{\infty}\frac{(-a)^k}{k!}\left(\frac{\partial^k t_2}{\partial r^k}\right)_{R,\theta}. \tag{13}$$

Substituting the Fourier representation (5) for $t_2$ into this equation yields

$$\begin{aligned}\frac{\partial^2 t_1}{\partial\theta^2} &= -\frac{R^2}{D_1} - \omega^2\left(\frac{aR}{2D_2} - \frac{a^2}{4D_2}\right)\\ &\quad -\omega^2\sum_{k=1}^{\infty}\frac{(-a)^k}{k!}\sum_{n=k}^{\infty}\alpha_n n(n-1)\ldots(n-k+1)R^{n-k}\cos(n\theta).\end{aligned} \tag{14}$$

Changing the order of summations over $n$ and $k$, using the binomial formula and the expression (7) for $\alpha_n$ give

$$\begin{aligned}\frac{\partial^2 t_1}{\partial\theta^2} &= -\frac{R^2}{D_1} - \omega^2\left(\frac{aR}{2D_2} - \frac{a^2}{4D_2}\right)\\ &\quad -\frac{\omega^2}{\pi}\sum_{n=1}^{\infty}(x^n-1)\cos(n\theta)\int_{\epsilon}^{2\pi-\epsilon}\cos(n\theta')t_1(\theta')\,\mathrm{d}\theta'.\end{aligned} \tag{15}$$

This integro-differential equation for $t_1$ can actually easily be transformed into an integral equation for $t_1$, by integrating successively two times, which leads to

$$t_1(\theta) = \frac{1}{2}\left(\frac{R^2}{D_1} + \omega^2\left(\frac{aR}{2D_2} - \frac{a^2}{4D_2}\right)\right)(\theta-\epsilon)(2\pi-\epsilon-\theta) + \frac{\omega^2}{\pi}\sum_{n=1}^{\infty}(x^n-1)\frac{\cos(n\theta)-\cos(n\epsilon)}{n^2}\int_{\epsilon}^{2\pi-\epsilon}\cos(n\theta')t_1(\theta')\,\mathrm{d}\theta', \tag{16}$$

or equivalently to

$$\psi(\theta) = (\theta-\epsilon)(2\pi-\epsilon-\theta) + \Omega\sum_{n=1}^{\infty}(x^n-1)\frac{\cos(n\theta)-\cos(n\epsilon)}{n^2}\int_{\epsilon}^{2\pi-\epsilon}\cos(n\theta')\psi(\theta')\,\mathrm{d}\theta', \tag{17}$$

where

$$\psi(\theta) \equiv \frac{2t_1(\theta)}{\omega^2 T}, \tag{18}$$

with $T$ defined in (10) and $\Omega \equiv \frac{\omega^2}{\pi}$. Note that (17) holds for $\theta \in [\epsilon, 2\pi-\epsilon]$. When there is no desorption (i.e., $\lambda = 0$), only the first term in (18) survives, yielding the classical result [30]

$$t_1(\theta) = \frac{R^2}{D_1}(\theta-\epsilon)(2\pi-\epsilon-\theta). \tag{19}$$

The same result is obtained for $a = 0$, since $x^n - 1 = (1-a/R)^n - 1 = 0$. The limit $a = 0$ is in fact equivalent to the limit $\lambda = 0$ because, after desorption, the particle immediately returns onto the circle ($a = 0$) as if it was never desorbed ($\lambda = 0$).

### 3.4 Exact Solution

Iterating the integral equation (17) shows that the solution $\psi(\theta)$ writes for $\theta \in [\epsilon, 2\pi-\epsilon]$:

$$\psi(\theta) = (\theta-\epsilon)(2\pi-\epsilon-\theta) + \sum_{n=1}^{\infty} d_n\big[\cos(n\theta)-\cos(n\epsilon)\big], \tag{20}$$

with the coefficients $d_n$ which satisfy

$$\sum_{n=1}^{\infty} d_n\big[\cos(n\theta)-\cos(n\epsilon)\big] = \Omega\sum_{n=1}^{\infty}\left(U_n + \sum_{n'=1}^{\infty} Q_{n,n'}d_{n'}\right)\big[\cos(n\theta)-\cos(n\epsilon)\big], \tag{21}$$

where we introduced

$$U_n \equiv \frac{x^n-1}{n^2}\int_{\epsilon}^{2\pi-\epsilon} d\theta'\cos(n\theta')(\theta'-\epsilon)(2\pi-\epsilon-\theta') = 4\frac{1-x^n}{n^4}\,\xi_n,$$
$$\xi_n \equiv (\pi-\epsilon)\cos(n\epsilon) + \frac{\sin(n\epsilon)}{n} \quad (n = 1, 2, \ldots), \tag{22}$$

and

$$Q_{n,n'} \equiv -\frac{1-x^n}{n^2} I_\epsilon(n, n') \quad (n, n' = 1, 2, \ldots), \tag{23}$$

with

$$
\begin{aligned}
I_\epsilon(n,n') &\equiv \int_\epsilon^{2\pi-\epsilon} \cos(n\theta)(\cos(n'\theta)-\cos(n'\epsilon))\,\mathrm{d}\theta \\
&= \left(1-\delta_{n,n'}\right)\left(2\frac{\cos(n'\epsilon)\sin(n\epsilon)}{n} - \frac{\sin((n'+n)\epsilon)}{n'+n} - \frac{\sin((n'-n)\epsilon)}{n'-n}\right) \\
&\quad + \delta_{n,n'}\left(\pi-\epsilon+\frac{\sin(2n\epsilon)}{2n}\right) \\
&= 2\left(1-\delta_{n,n'}\right)\frac{\cos(n\epsilon)\frac{\sin(n'\epsilon)}{n'} - \cos(n'\epsilon)\frac{\sin(n\epsilon)}{n}}{n^2-n'^2}\,n'^2 + \delta_{n,n'}\left(\pi-\epsilon+\frac{\sin(2n\epsilon)}{2n}\right).
\end{aligned}
\tag{24}
$$

Since (21) should be satisfied for any $\theta \in [\epsilon, 2\pi-\epsilon]$, one gets $\mathbf{d} = \Omega(U + Q\mathbf{d})$, from which

$$
d_n = \Omega\left[(I-\Omega Q)^{-1}U\right]_n \quad (n=1,2,\ldots). \tag{25}
$$

Since

$$
(I-\Omega Q)^{-1} = \sum_{i=0}^{\infty}(\Omega Q)^i, \tag{26}
$$

(20) with the $d_n$ given by (25) can be seen as a series in powers of $\Omega$, whose $n$-th order coefficient is explicitly written in terms of the $n$-th power of the matrix $Q$.

Note that the first term in (20) can also be expended in a Fourier series

$$
\sum_{n=1}^{\infty} e_n\left[\cos(n\theta)-\cos(n\epsilon)\right] = \begin{cases} (\theta-\epsilon)(2\pi-\epsilon-\theta), & \epsilon<\theta<2\pi-\epsilon, \\ 0, & \text{otherwise}, \end{cases} \tag{27}
$$

where the coefficients $e_n$ are obtained by multiplying this equation by $\cos m\theta$ and integrating from 0 to $2\pi$:

$$
e_n = -\frac{4}{\pi n^2}\xi_n \quad (n=1,2,\ldots). \tag{28}
$$

Once the $d_n$ determined, the search time $\langle t_1\rangle$ is

$$
\langle t_1\rangle \equiv \frac{1}{2\pi}\int_0^{2\pi} t_1(\theta)\,d\theta = \frac{\omega^2 T}{4\pi}\int_\epsilon^{2\pi-\epsilon}\psi(\theta)\,d\theta = \frac{\omega^2 T}{2\pi}\left\{\frac{2}{3}(\pi-\epsilon)^3 - \sum_{n=1}^{\infty} d_n\xi_n\right\}. \tag{29}
$$

### 3.5 Approximate Solution

While the previous expression of $t_1$ is exact, it is not fully explicit, since it requires either the inversion of the matrix $I-\Omega Q$ or the calculation of all the powers of $Q$. We give here an approximation of $(I-\Omega Q)^{-1}$, which in turn provides a convenient and fully explicit representation of $t_1$. As shown numerically (see Figs. 2, 3, 4 and Sect. 5 for more details about numerical methods), this approximation of $t_1$ proves to be in quantitative agreement with the exact expression for a wide range of parameters.

This approximation relies on the fact that, in the small target size limit $\epsilon \to 0$, the matrix $Q$ is diagonal, which mirrors the orthogonality of the $\{\cos(n\theta)\}_n$ on $[0, 2\pi]$. More precisely, one has from (23), (24):

$$
Q_{m,n} = \delta_{m,n}Q_{n,n} + \mathcal{O}(\epsilon^3), \tag{30}
$$

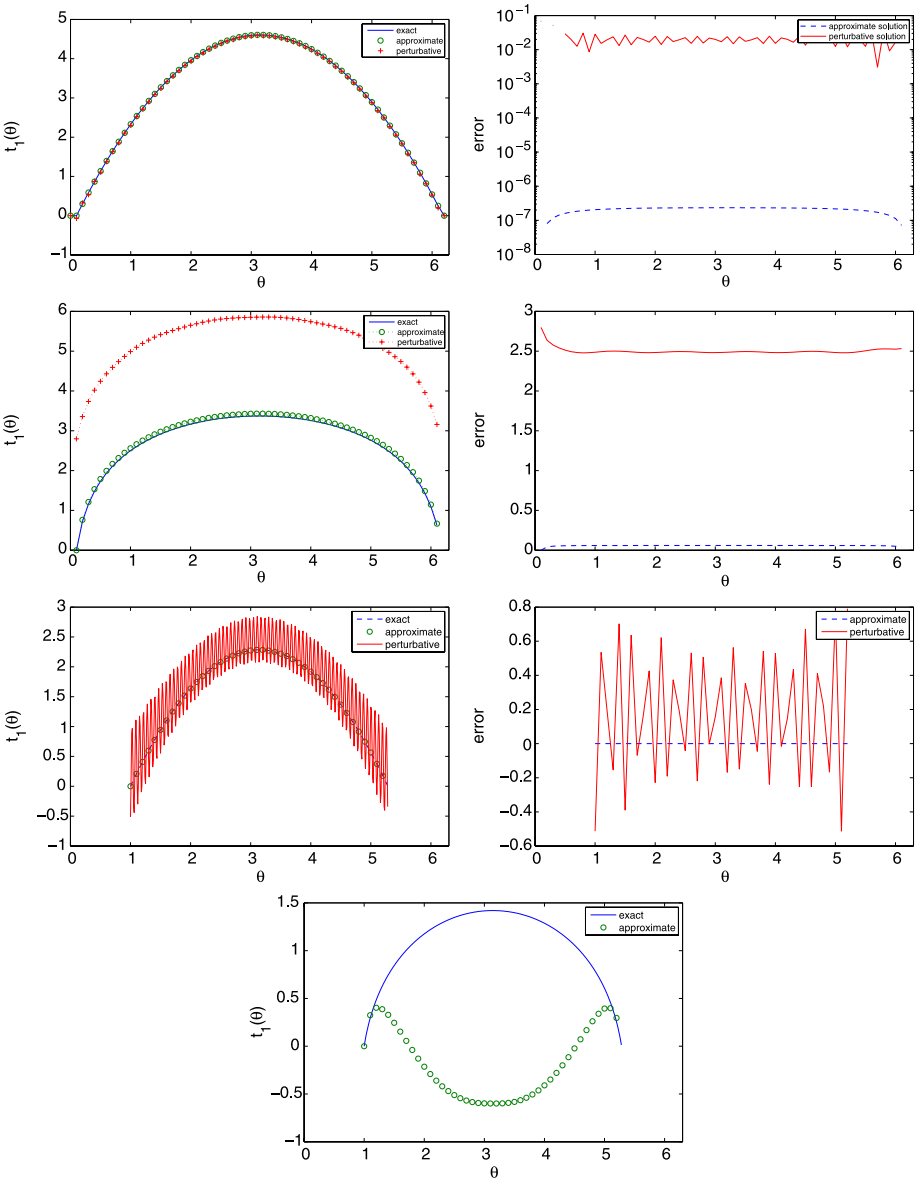


**Fig. 2** (Color online) Comparison between three approaches for computing $t_1(\theta)$ in 2D: the exact solution (20), (25), the approximation (32) and the perturbative formula (A.15), with $D_2 = 1$, $a = 0.01$. In the *first row*, the other parameters are: $\epsilon = 0.1$, $\lambda = 1$, and the series are truncated to $N = 100$. *On the right*, the absolute error between the exact solution and the approximation (*dashed blue curve*) and between the exact solution and the perturbative formula (*solid red curve*). The approximation is very accurate indeed. In the *second row*, the parameters are: $\epsilon = 0.1$, $\lambda = 1000$, and the series are truncated to $N = 100$ for the exact and approximate solutions, and to $N = 1000$ for the perturbative solution. One can see that the perturbative solution is inaccurate for large values of $\lambda$, while the maximal relative error of the approximate solution is below 2%. In the *third row*, the parameters are: $\epsilon = 1$, $\lambda = 1$, and the series are truncated to $N = 100$. The perturbative solution is evidently not applicable. In the *last row*, the parameters are: $\epsilon = 1$, $\lambda = 1000$, and the series are truncated to $N = 100$. In this case, the approximate solution significantly deviates from the exact one (providing mostly negative values). The perturbative solution is completely invalid (not shown)

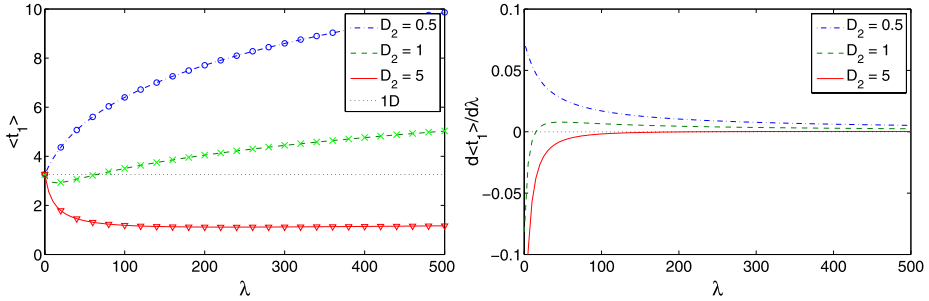


**Fig. 3** (Color online) *Left*: In 2D, the mean time $\langle t_1 \rangle$ computed through (25), (29) with $N = 100$ as a function of the desorption rate $\lambda$ for three values of $D_2$: $D_2 = 0.5$ (*dot-dashed blue line*), $D_2 = 1$ (*dashed green line*), and $D_2 = 5$ (*solid red line*). The other parameters are: $a = 0.1$ and $\epsilon = 0.01$. When $D_2 < D_{2,\mathrm{crit}} \approx 0.6348...$ (the first case), $\langle t_1 \rangle$ monotonously increases with $\lambda$ so that there is no optimal value. In two other cases, $D_2 > D_{2,\mathrm{crit}}$, and $\langle t_1 \rangle$ starts first to decrease with $\lambda$, passes through a minimum (the optimal value) and monotonously increases. Symbols show the approximate mean time computed through (31), (29). One can see that the approximation accurate enough even for large values of $\lambda$. *Right*: The derivative $\frac{d\langle t_1 \rangle}{d\lambda}$ defined by (35) for the same parameters

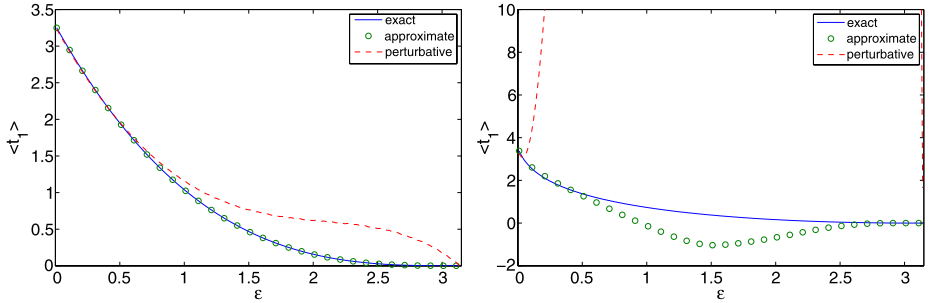


**Fig. 4** In 2D, the mean time $\langle t_1 \rangle$ as a function of $\epsilon$, with $D_2 = 1$, $a = 0.01$, and $\lambda = 1$ (*left*) or $\lambda = 1000$ (*right*). The exact computation through (25), (29) is compared to the approximation (31), (29) and to the perturbative approach. In all cases, the series are truncated to $N = 100$. For small $\lambda$ ($\lambda = 1$), the approximate solution is very close to the exact one, while the perturbative solution is relatively close for $\epsilon$ up to 1. In turn, for large $\lambda$ ($\lambda = 1000$), the approximate solution shows significant deviations for the intermediate values of $\epsilon$, while the perturbative solution is not applicable at all

and keeping only the leading term of this expansion yields

$$d_n \approx \Omega(1 - \Omega Q_{n,n})^{-1} U_n, \tag{31}$$

from which we obtain the desired approximation:

$$\psi(\theta) \approx (\theta - \epsilon)(2\pi - \epsilon - \theta) + 4\Omega \sum_{n=1}^{\infty} (\cos(n\theta) - \cos(n\epsilon)) \times \frac{n(\pi - \epsilon)\cos(n\epsilon) + \sin(n\epsilon)}{n^3} \frac{1 - x^n}{n^2 + \Omega(1 - x^n) I_\epsilon(n, n)}. \tag{32}$$

This yields an approximation for the search time:

$$\langle t_1\rangle \approx \frac{\omega^2 T}{2\pi}\left\{\frac{2}{3}(\pi-\epsilon)^3 - 4\Omega\sum_{n=1}^{\infty}\frac{1-x^n}{n^2}\frac{\left((\pi-\epsilon)\cos(n\epsilon)+\frac{\sin(n\epsilon)}{n}\right)^2}{n^2+\Omega(1-x^n)\left(\pi-\epsilon+\frac{\sin(2n\epsilon)}{2n}\right)}\right\}. \tag{33}$$

### 3.6 Variations of the Search Time $\langle t_1\rangle$ with the Desorption Rate $\lambda$

In this section, we answer two important questions. When are bulk excursions favorable, meaning enabling to reduce the search time (with respect to the situation with no bulk excursion corresponding to $\lambda = 0$)? If so, is there an optimal value of the desorption rate $\lambda$ minimizing the search time?

#### *3.6.1 When are Bulk Excursions Beneficial to the Search?*

This question can be investigated by studying the sign of the derivative $\frac{\partial\langle t_1\rangle}{\partial\lambda}$ at $\lambda = 0$. The mean search time from (29) can also be written as

$$\langle t_1\rangle = \frac{R^4}{2\pi^2 D_1^2}\big(1+\lambda\eta\big)\left[\frac{2\pi D_1}{3R^2}(\pi-\epsilon)^3 - \lambda\big(\xi\cdot(I+\lambda\tilde{Q})^{-1}U\big)\right], \tag{34}$$

where $\tilde{Q} = -Q\frac{R^2}{\pi D_1}$, $\eta = \frac{2aR-a^2}{4D_2}$. The derivative of $\langle t_1\rangle$ with respect to $\lambda$ is then

$$\frac{\partial\langle t_1\rangle}{\partial\lambda} = \frac{R^4\eta}{2\pi^2 D_1^2}\left[\frac{2\pi D_1}{3R^2}(\pi-\epsilon)^3 - \left(\xi\cdot\frac{(\eta^{-1}+2\lambda)I+\lambda^2\tilde{Q}}{(I+\lambda\tilde{Q})^2}U\right)\right]. \tag{35}$$

If the derivative is negative at $\lambda = 0$, i.e.

$$\eta\frac{2\pi D_1}{3R^2}(\pi-\epsilon)^3 < \big(\xi\cdot U\big), \tag{36}$$

bulk excursions are beneficial to the search. This inequality determines the critical value for the bulk diffusion coefficient $D_{2,\mathrm{crit}}$ (which enters through $\eta$), above which bulk excursions are beneficial:

$$\begin{aligned}\frac{D_1}{D_{2,\mathrm{crit}}} &= \frac{6R^2(\xi\cdot U)}{\pi(\pi-\epsilon)^3(2aR-a^2)}\\ &= \frac{24}{\pi(\pi-\epsilon)^3(1-x^2)}\sum_{n=1}^{\infty}\frac{1-x^n}{n^4}\left[(\pi-\epsilon)\cos(n\epsilon)+\frac{\sin(n\epsilon)}{n}\right]^2.\end{aligned} \tag{37}$$

Two comments are in order:

(i) Interestingly, this ratio depends only on $a/R$ and $\epsilon$. In the limit of $\epsilon\to 0$, one gets

$$\frac{D_1}{D_{2,\mathrm{crit}}} \approx \frac{24}{\pi^2(1-x^2)}\sum_{n=1}^{\infty}\frac{1-x^n}{n^4}. \tag{38}$$

Taking next the limit $a/R\to 0$ finally yields:

$$\frac{D_1}{D_{2,\mathrm{crit}}} \approx \frac{12\zeta(3)}{\pi^2} \approx 1.4615, \tag{39}$$

where $\zeta$ stands for the Riemann $\zeta$-function.

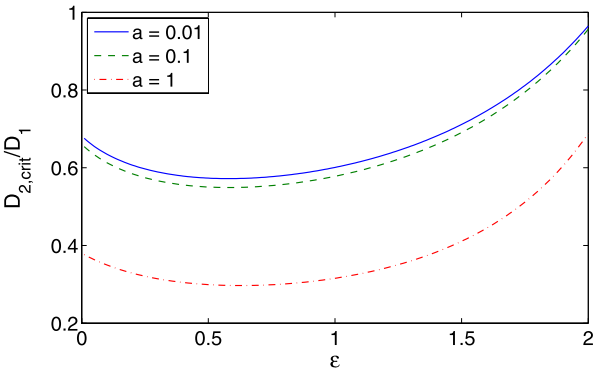


**Fig. 5** $D_{2,\mathrm{crit}}$ as a function of $\epsilon$ is computed from (37) in 2D for three values of $a/R$: 0.01, 0.1, and 1. When $\epsilon$ approaches $\pi$ (the whole surface becomes absorbing), $D_{2,\mathrm{crit}}$ diverges (not shown). In fact, in this limit, there is no need for a bulk excursion because the target will be found immediately by the surface diffusion

(ii) The dependence of the r.h.s. of (37) with $\epsilon$ is not trivial (Fig. 5). Indeed it can be proved to have a maximum with respect to $\epsilon$, which can be understood intuitively as follows: in the vicinity of $\epsilon = 0$, increasing $\epsilon$ makes the constraint less stringent since the target can be reached directly from the bulk; in the opposite limit $\epsilon \to \pi$, the constraint on $D_1/D_2$ has to tend to 0 since the target is found immediately from the surface. Quantitatively, in the physical limit $a \to 0$, one finds that, as soon as $D_2/D_1 > (D_{2,\mathrm{crit}}/D_1) \approx 0.68\ldots$, bulk excursions can be beneficial.

### *3.6.2 When is there an Optimal Value of the Desorption Rate λ Minimizing the Search Time?*

If the reaction time $\langle t_1 \rangle$ is a decreasing function of the desorption rate $\lambda$, the bulk excursions are "too favorable", and the best search strategy is obtained for $\lambda \to \infty$ (purely bulk search). For the reaction time to be an optimizable function of $\lambda$, the derivative $\frac{d\langle t_1 \rangle}{d\lambda}$ has to be positive at some $\lambda$. This necessary and sufficient condition remains formal and requires numerical analysis of (35). A simple *sufficient* condition can be used instead by demanding that the search time at zero desorption rate is less than the search time at infinite desorption rate:

$$\langle t_1(\lambda = 0) \rangle < \langle t_1(\lambda \to \infty) \rangle. \tag{40}$$

This writes in the physically relevant limit $a \ll R$ (using the result of [35]):

$$\frac{D_1}{D_2} > \frac{(\pi - \epsilon)^3}{3\pi c(\epsilon)}, \quad \text{with } c(\epsilon) \equiv \frac{1}{\pi\sqrt{2}} \int_0^{\pi-\epsilon} \frac{u \sin(u/2)}{\sqrt{\cos(u) + \cos(\epsilon)}}\, \mathrm{d}u. \tag{41}$$

Finally, combining (37), (41), the search time is found to be an optimizable function of $\lambda$ in the limit $a \ll R$ if

$$\frac{(\pi - \epsilon)^3}{3\pi c(\epsilon)} < \frac{D_1}{D_2} < \frac{12}{\pi(\pi - \epsilon)^3} \sum_{n=1}^{\infty} \frac{1}{n^3} \left[ (\pi - \epsilon)\cos(n\epsilon) + \frac{\sin(n\epsilon)}{n} \right]^2. \tag{42}$$

Knowing that $c(\epsilon) = \ln(2/\epsilon) + \mathcal{O}(\epsilon)$, (42) writes in the small $\epsilon$ limit:

$$\frac{\pi^2}{3\ln(2/\epsilon)} < \frac{D_1}{D_2} < \frac{12\zeta(3)}{\pi^2}, \tag{43}$$

which summarizes the conditions for the search time to be an optimizable function of $\lambda$. This case is illustrated in Fig. 10.

## 4 3D Case

In this section, the confining domain is a sphere of radius $R$ and the target is the region on the boundary defined by $\theta \in [0, \epsilon]$, where $\theta$ is the elevation angle.

### 4.1 Basic Equations

The 3D analogs of (1), (2) read as

$$\frac{D_1}{R^2}\left(\frac{\partial^2 t_1}{\partial \theta^2} + \frac{1}{\tan\theta}\frac{\partial t_1}{\partial \theta}\right) + \lambda[t_2(R-a,\theta) - t_1(\theta)] = -1 \quad \text{for } \theta \in [\epsilon, \pi], \tag{44}$$

$$D_2\left(\frac{\partial^2}{\partial r^2} + \frac{2}{r}\frac{\partial}{\partial r} + \frac{1}{r^2}\frac{\partial^2}{\partial \theta^2} + \frac{1}{r^2}\frac{1}{\tan\theta}\frac{\partial}{\partial \theta}\right) t_2(r,\theta) = -1. \tag{45}$$

These equations have to be completed by two boundary conditions:

$$t_2(R,\theta) = t_1(\theta), \tag{46}$$

$$t_1(\theta) = 0 \quad \text{for } \theta \in [0, \epsilon], \tag{47}$$

which respectively describe the adsorption events and express that the target is an absorbing region of the sphere.

### 4.2 Integral Equation for $t_1$

One can search for a solution in the following form

$$t_2(r,\theta) = \alpha_0 - \frac{r^2}{6D_2} + \sum_{n=1}^{\infty} \alpha_n r^n P_n(\cos\theta), \tag{48}$$

where $P_n$ stands for the Legendre polynomial of order $n$. Using the orthonormality of Legendre polynomials, the projection of $t_2(R,\theta)$ on $P_m$ writes

$$\int_0^{\pi} \sin\theta\, P_m(\cos\theta) t_2(R,\theta)\, \mathrm{d}\theta = 2\left(\alpha_0 - \frac{R^2}{6D_2}\right)\delta_{m,0} + \frac{2\alpha_m R^m}{2m+1}. \tag{49}$$

Knowing that

$$t_2(R,\theta) = \begin{cases} t_1(\theta) & \text{if } \theta \in [\epsilon, \pi], \\ 0 & \text{if } \theta \in [0, \epsilon], \end{cases} \tag{50}$$

the $\alpha_n$ can be written in terms of $t_1(\theta)$ as

$$\begin{aligned} \alpha_0 - \frac{R^2}{6D_2} &= \frac{1}{2}\int_{\epsilon}^{\pi} \sin\theta\, t_1(\theta)\, \mathrm{d}\theta, \\ \alpha_n R^n &= \frac{2n+1}{2}\int_{\epsilon}^{\pi} \sin\theta\, P_n(\cos\theta)\, t_1(\theta)\, \mathrm{d}\theta \quad \text{if } n \geq 1. \end{aligned} \tag{51}$$

Taylor expanding the r.h.s. of

$$\frac{\partial^2 t_1}{\partial \theta^2} + \frac{1}{\tan\theta}\frac{\partial t_1}{\partial \theta} = -\frac{R^2}{D_1} - \omega^2[t_2(R-a,\theta) - t_2(R,\theta)] \tag{52}$$

leads to

$$\frac{\partial^2 t_1}{\partial\theta^2}+\frac{1}{\tan\theta}\frac{\partial t_1}{\partial\theta}=-\frac{R^2}{D_1}-\omega^2\sum_{k=1}^{\infty}\frac{(-a)^k}{k!}\left(\frac{\partial^k t_2}{\partial r^k}\right)_{R,\theta}. \tag{53}$$

Using (48) for $t_2$ yields

$$\begin{aligned}\frac{\partial^2 t_1}{\partial\theta^2}+\frac{1}{\tan\theta}\frac{\partial t_1}{\partial\theta}=&-\frac{R^2}{D_1}-\omega^2\left(\frac{aR}{3D_2}-\frac{a^2}{6D_2}\right)\\&-\omega^2\sum_{k=1}^{\infty}\frac{(-a)^k}{k!}\sum_{n=k}^{\infty}\alpha_n n(n-1)\dots(n-k+1)R^{n-k}P_n(\cos\theta).\end{aligned} \tag{54}$$

Changing the order of summations over $n$ and $k$ and using the binomial formula and (51) for $\alpha_n$ finally give

$$\begin{aligned}\frac{\partial^2 t_1}{\partial\theta^2}+\frac{1}{\tan\theta}\frac{\partial t_1}{\partial\theta}=&-\frac{R^2}{D_1}-\omega^2\left(\frac{aR}{3D_2}-\frac{a^2}{6D_2}\right)-\frac{\omega^2}{2}\sum_{n=1}^{\infty}(x^n-1)P_n(\cos\theta)(2n+1)\\&\times\int_{\epsilon}^{\pi}\sin\theta' P_n(\cos\theta')t_1(\theta')\,\mathrm{d}\theta',\end{aligned} \tag{55}$$

where, as in previous section, $x\equiv 1-\frac{a}{R}$. This integro-differential equation for $t_1$ can actually easily be transformed into an integral equation for $t_1$, by integrating successively two times. Indeed, multiplying first both members of (55) by $\sin\theta$ and integrating between $\pi$ and $\theta$ gives

$$\begin{aligned}\sin\theta\, t_1'(\theta)=&\left[\frac{R^2}{D_1}+\omega^2\left(\frac{aR}{3D_2}-\frac{a^2}{6D_2}\right)\right](\cos\theta+1)+\frac{\omega^2}{2}\sum_{n=1}^{\infty}(x^n-1)(P_{n+1}(\cos\theta)\\&-P_{n-1}(\cos\theta))\int_{\epsilon}^{\pi}\sin\theta' P_n(\cos\theta')t_1(\theta')\,\mathrm{d}\theta',\end{aligned} \tag{56}$$

where we have used

$$\int P_n(x)\,\mathrm{d}x=-\frac{1}{n(n+1)}(1-x^2)P_n'(x)=\frac{1}{2n+1}(P_{n+1}(x)-P_{n-1}(x)). \tag{57}$$

Dividing (56) by $\sin\theta$ and integrating between $\epsilon$ and $\theta$ finally leads to

$$\begin{aligned}t_1(\theta)=&2\left(\frac{R^2}{D_1}+\omega^2\left(\frac{aR}{3D_2}-\frac{a^2}{6D_2}\right)\right)\ln\left(\frac{\sin(\theta/2)}{\sin(\epsilon/2)}\right)\\&+\frac{\omega^2}{2}\sum_{n=1}^{\infty}(x^n-1)\frac{2n+1}{n(n+1)}(P_n(\cos\theta)-P_n(\cos\epsilon))\int_{\epsilon}^{\pi}\sin\theta' P_n(\cos\theta')t_1(\theta')\,\mathrm{d}\theta',\end{aligned}$$

where we have again used (57), or equivalently to

$$\psi(\theta) = \ln\left(\frac{1-\cos\theta}{1-\cos\epsilon}\right) + \Omega \sum_{n=1}^{\infty} (x^n - 1)\frac{2n+1}{n(n+1)}\big(P_n(\cos\theta) - P_n(\cos\epsilon)\big)$$

$$\times \int_{\epsilon}^{\pi} \sin(\theta')\, P_n(\cos\theta')\psi(\theta')\, \mathrm{d}\theta', \tag{58}$$

with the following definitions

$$\psi(\theta) \equiv \frac{t_1(\theta)}{\omega^2 T}, \qquad T \equiv \frac{1}{\lambda} + \frac{R^2 - (R-a)^2}{6D_2}, \qquad \Omega \equiv \frac{\omega^2}{2} \tag{59}$$

in this 3D case.

### 4.3 Exact Solution

Iterating the integral equation (58) shows that the solution $\psi(\theta)$ writes for $\theta \in [\epsilon, \pi]$:

$$\psi(\theta) = \ln\left(\frac{1-\cos\theta}{1-\cos\epsilon}\right) + \sum_{n=1}^{\infty} d_n\big[P_n(\cos\theta) - P_n(\cos\epsilon)\big], \tag{60}$$

with the coefficients $d_n$ which satisfy

$$\sum_{n=1}^{\infty} d_n\big[P_n(\cos\theta) - P_n(\cos\epsilon)\big] = \Omega \sum_{n=1}^{\infty}\left(U_n + \sum_{n'=1}^{\infty} Q_{n,n'} d_{n'}\right)\big[P_n(\cos\theta) - P_n(\cos\epsilon)\big], \tag{61}$$

where we introduced the new definitions

$$U_n \equiv \frac{(x^n-1)(2n+1)}{n(n+1)} \int_{\epsilon}^{\pi} \mathrm{d}\theta' \sin(\theta') P_n(\cos\theta') \ln\left(\frac{1-\cos\theta'}{1-\cos\epsilon}\right) = \frac{(1-x^n)(2n+1)}{n^2(n+1)^2}\, \xi_n,$$

$$\xi_n \equiv \left(1 + \frac{n\cos\epsilon}{n+1}\right) P_n(\cos\epsilon) + \frac{P_{n-1}(\cos\epsilon)}{n+1} \quad (n = 1, 2, \ldots), \tag{62}$$

and

$$Q_{n,n'} \equiv -\frac{(1-x^n)(2n+1)}{n(n+1)} I_{\epsilon}(n, n') \quad (n, n' = 1, 2, \ldots), \tag{63}$$

with

$$I_{\epsilon}(n, n') \equiv \int_{-1}^{\cos\epsilon} P_n(u)\big(P_{n'}(u) - P_{n'}(\cos\epsilon)\big)\, \mathrm{d}u. \tag{64}$$

In Appendix C, we compute this integral explicitly.

Since (58) should be satisfied for any $\theta$, one gets $\mathbf{d} = \Omega(U + Q\mathbf{d})$, from which

$$d_n = \Omega\big[(I - \Omega Q)^{-1} U\big]_n \quad (n = 1, 2, \ldots). \tag{65}$$

As in 2D, using the series expansion of $(I - \Omega Q)^{-1}$, (65) can be seen as a series in powers of $\Omega$, whose $n$-th order coefficient can be explicitly written in terms of the $n$-th power of the matrix $Q$.

Note that the first term in (60) can also be represented as a series

$$\sum_{n=1}^{\infty} e_n \big[P_n(\cos\theta) - P_n(\cos\epsilon)\big] = \begin{cases} \ln\big(\frac{1-\cos\theta}{1-\cos\epsilon}\big), & \epsilon < \theta < \pi - \epsilon, \\ 0, & \text{otherwise}, \end{cases} \tag{66}$$

where the coefficients $e_n$ are obtained by multiplying this equation by $P_n(\cos\theta)\sin\theta$ and integrating from 0 to $\pi$:

$$e_n = -\frac{2n+1}{2n(n+1)}\xi_n. \tag{67}$$

Once the $d_n$ determined, the search time $\langle t_1 \rangle$ can be written as

$$\langle t_1 \rangle \equiv \frac{\omega^2 T}{2} \int_{\epsilon}^{\pi} d\theta \ \sin\theta \ \psi(\theta) = \frac{\omega^2 T}{2} \left\{ 2\ln\left(\frac{2}{1-\cos\epsilon}\right) - (1+\cos\epsilon) - \sum_{n=1}^{\infty} d_n \xi_n \right\}. \tag{68}$$

### 4.4 Perturbative Solution

The first terms of a perturbative expansion with respect to $\epsilon$ can easily be obtained from the previous exact solution. At leading order in $\epsilon$, we have

$$\begin{aligned} U_n &= U_n^{(0)} + O(\epsilon) = \frac{2(1-x^n)(2n+1)}{n^2(n+1)^2} + O(\epsilon), \\ Q_{m,n} &= Q_{m,n}^{(0)} + O(\epsilon) = -\frac{2(1-x^n)}{n(n+1)}\delta_{m,n} + O(\epsilon), \end{aligned} \tag{69}$$

from which

$$d_n = \Omega\big[(I - \Omega Q^{(0)})^{-1} U^{(0)}\big]_n + O(\epsilon) = \frac{2\Omega}{n(n+1)} \frac{(1-x^n)(2n+1)}{n(n+1) + 2\Omega(1-x^n)} + O(\epsilon). \tag{70}$$

One finds therefore

$$\begin{aligned} \psi(\theta) &= -2\ln\epsilon + 2\ln\left(2\sin(\theta/2)\right) \\ &\quad - 2\Omega \sum_{n=1}^{\infty} (1-x^n) \frac{2n+1}{n(n+1)} \frac{1 - P_n(\cos\theta)}{n(n+1) + 2\Omega(1-x^n)} + O(\epsilon). \end{aligned} \tag{71}$$

Averaging over $\theta$, it finally yields:

$$\langle t_1 \rangle \approx \omega^2 T \left\{ -2\ln(\epsilon/2) - 1 - 2\Omega \sum_{n=1}^{\infty} \frac{2n+1}{n(n+1)} \frac{(1-x^n)}{n(n+1) + 2\Omega(1-x^n)} + O(\epsilon) \right\}. \tag{72}$$

This result was given in [42] without derivation.

### 4.5 Approximate Solution

As earlier for the 2D case, an approximate solution can be derived. As shown numerically (see Figs. 6, 7, 8 and Sect. 5 for more details about numerical methods), this approximation of $t_1$ proves to be in quantitative agreement with the exact expression for a wide range of parameters.

This approximation relies on the fact that, in the small target size limit $\epsilon \to 0$, the matrix $Q$ is diagonal, which in turn mirrors the orthogonality of $\{P_n(\cos\theta)\}_n$ on $[0,\pi]$. More precisely, one has

$$Q_{m,n} = \delta_{m,n} Q_{n,n} + \mathcal{O}(\epsilon^4), \tag{73}$$

and keeping only the leading term of this expansion yields

$$d_n \approx \Omega(1-\Omega Q_{n,n})^{-1} U_n, \tag{74}$$

from which

$$\psi(\theta) \approx \ln\left(\frac{1-\cos\theta}{1-\cos\epsilon}\right) + \Omega \sum_{n=1}^{\infty} (1-x^n)\frac{2n+1}{n(n+1)}(P_n(\cos\theta) - P_n(\cos\epsilon)) \times \frac{(1+\frac{n\cos\epsilon}{n+1})P_n(\cos\epsilon) + \frac{P_{n-1}(\cos\epsilon)}{n+1}}{n(n+1) + \Omega(1-x^n)(2n+1)I_\epsilon(n,n)}. \tag{75}$$

The mean time $\langle t_1 \rangle$ is then approximated as

$$\langle t_1 \rangle \approx \omega^2 T \left\{ \ln\left(\frac{2}{1-\cos\epsilon}\right) - \frac{1+\cos\epsilon}{2} - \frac{\Omega}{2}\sum_{n=1}^{\infty} \frac{(1-x^n)(2n+1)}{n(n+1)} \frac{[(1+\frac{n\cos\epsilon}{n+1})P_n(\cos\epsilon) + \frac{P_{n-1}(\cos\epsilon)}{n+1}]^2}{n(n+1) + \Omega(1-x^n)(2n+1)I_\epsilon(n,n)} \right\}, \tag{76}$$

where $I_\epsilon$ is defined by (64).

### 4.6 Variations of the Search Time $\langle t_1 \rangle$ with the Desorption rate $\lambda$

We investigate here as in the 2D case the dependence of $\langle t_1 \rangle$ on $\lambda$.

#### *4.6.1 When are Bulk Excursions Beneficial to the Search?*

The sign of $\frac{\partial \langle t_1 \rangle}{\partial \lambda}$ at $\lambda = 0$ is conveniently studied by rewriting (68) as

$$\langle t_1 \rangle = \frac{R^4}{4D_1^2}(1+\lambda\eta)\left\{ \frac{4D_1}{R^2}\left[ \ln\left(\frac{2}{1-\cos\epsilon}\right) - \frac{1+\cos\epsilon}{2}\right] - \lambda\left(\xi \cdot (I+\lambda\tilde{Q})^{-1}U\right)\right\}, \tag{77}$$

where $\tilde{Q} = -Q\frac{R^2}{2D_1}$ and $\eta = \frac{2aR-a^2}{6D_2}$. The derivative of $\langle t_1 \rangle$ with respect to $\lambda$ is then

$$\frac{\partial \langle t_1 \rangle}{\partial \lambda} = \frac{R^4\eta}{4D_1^2}\left\{ \left[ \ln\left(\frac{2}{1-\cos\epsilon}\right) - \frac{1+\cos\epsilon}{2}\right] - \left(\xi \cdot \frac{(\eta^{-1}+2\lambda)I + \lambda^2\tilde{Q}}{(I+\lambda\tilde{Q})^2}U\right)\right\}. \tag{78}$$

If the above derivative is negative at $\lambda = 0$, i.e.

$$\frac{4D_1}{R^2}\left( \ln\left(\frac{2}{1-\cos\epsilon}\right) - \frac{1+\cos\epsilon}{2}\right) < \frac{(\xi \cdot U)}{\eta}, \tag{79}$$

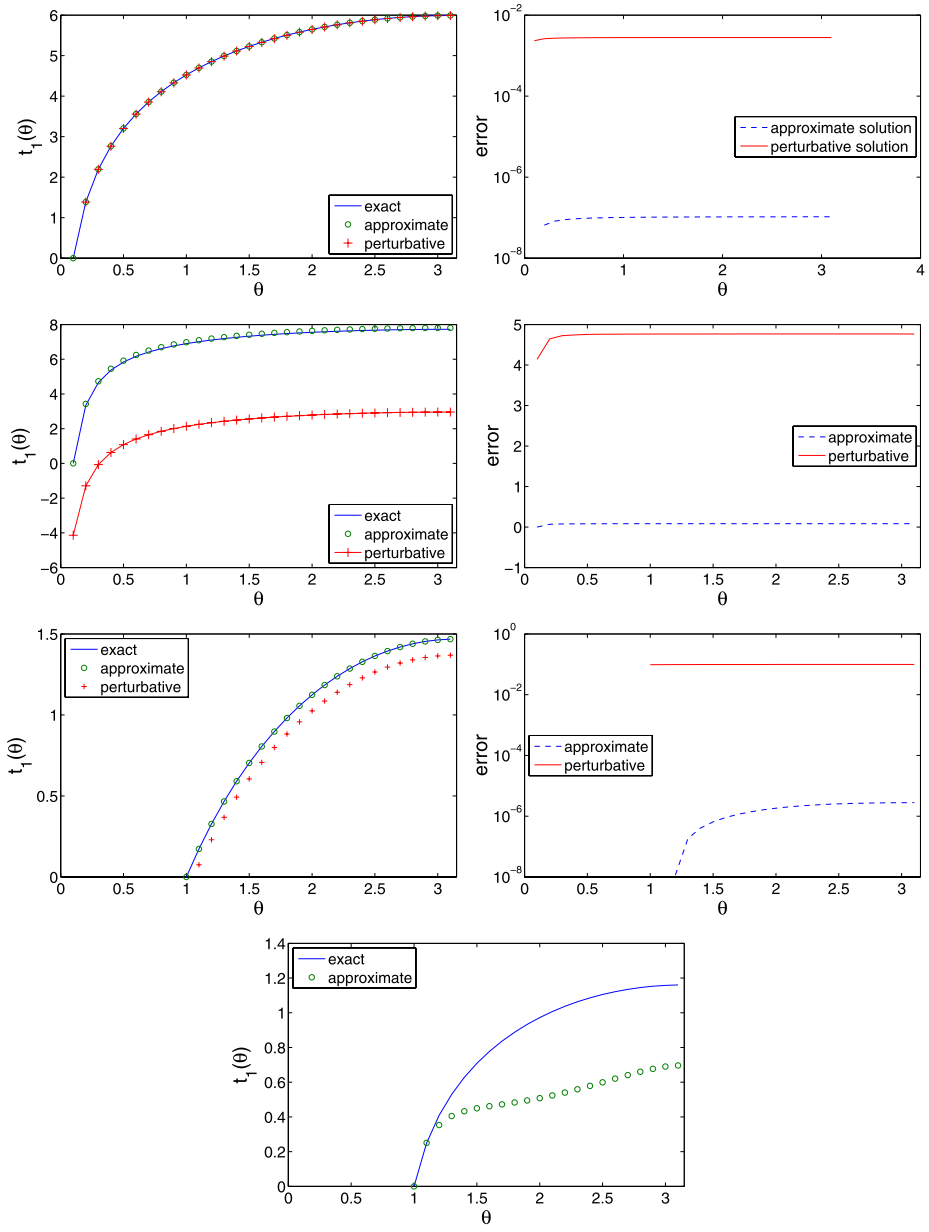


**Fig. 6** (Color online) Comparison between three approaches for computing $t_1(\theta)$ in 3D: the exact solution (60), (65), the approximation (75) and the perturbative formula (71), with $D_2 = 1$, $a = 0.01$. In the *first row*, the other parameters are: $\epsilon = 0.1$, $\lambda = 1$, and the series are truncated to $N = 100$. *On the right*, the absolute error between the exact solution and the approximation (*dashed blue curve*) and between the exact solution and the perturbative formula (*solid red curve*). The approximation is very accurate indeed. In the *second row*, the parameters are: $\epsilon = 0.1$, $\lambda = 1000$, and the series are truncated to $N = 100$. One can see that the perturbative solution is inaccurate for large values of $\lambda$, while the maximal relative error of the approximate solution is still small. In the *third row*, the parameters are: $\epsilon = 1$, $\lambda = 1$, and the series are truncated to $N = 100$. The perturbative solution is inaccurate as expected for large $\epsilon$. In the *last row*, the parameters are: $\epsilon = 1$, $\lambda = 1000$, and the series are truncated to $N = 100$. In this case, the approximate solution deviates from the exact one for. The perturbative solution is negative and not shown

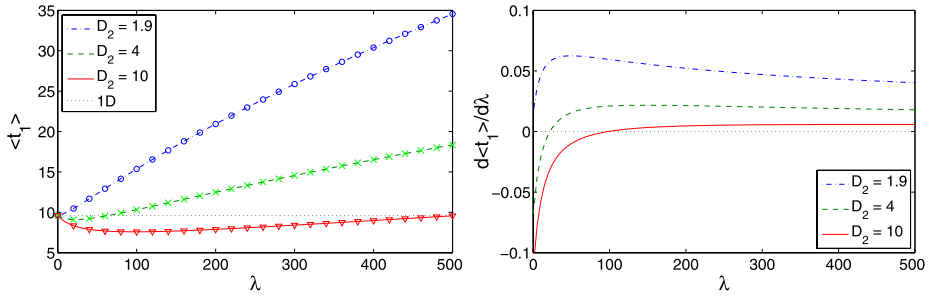


**Fig. 7** (Color online) *Left*: In 3D, the mean time $\langle t_1 \rangle$ computed through (65), (68) with $N = 100$ as a function of the desorption rate $\lambda$ for three values of $D_2$: $D_2 = 1.9$ (*dot-dashed blue line*), $D_2 = 4$ (*dashed green line*), and $D_2 = 10$ (*solid red line*). The other parameters are: $a = 0.1$ and $\epsilon = 0.01$. When $D_2 < D_{2,\mathrm{crit}} \approx 1.9997...$ (the first case), $\langle t_1 \rangle$ monotonously increases with $\lambda$ so that there is no optimal value. In two other cases, $D_2 > D_{2,\mathrm{crit}}$, and $\langle t_1 \rangle$ starts first to decrease with $\lambda$, passes through a minimum (the optimal value) and then increases. *Symbols* show the approximate mean time computed through (76). One can see that the approximation accurate enough even for large values of $\lambda$. *Right*: The derivative $\frac{d\langle t_1 \rangle}{d\lambda}$ defined by (78) for the same parameters

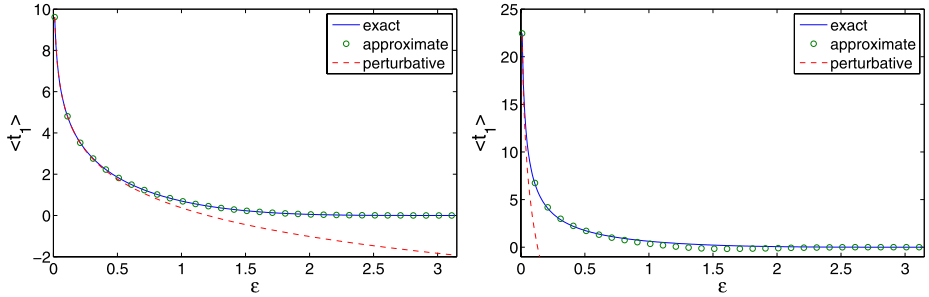


**Fig. 8** In 3D, the mean time $\langle t_1 \rangle$ as a function of $\epsilon$, with $D_2 = 1$, $a = 0.01$, and $\lambda = 1$ (*left*) or $\lambda = 1000$ (*right*). The exact computation through (65), (68) is compared to the approximation (76) and to the perturbative approach. In all cases, the series are truncated to $N = 100$. For small $\lambda$ ($\lambda = 1$), the approximate solution is very close to the exact one, while the perturbative solution is relatively close for $\epsilon$ up to 1. In turn, for large $\lambda$ ($\lambda = 1000$), the approximate solution shows significant deviations for the intermediate values of $\epsilon$, while the perturbative solution is not applicable at all

bulk excursions are beneficial to the search. This inequality determines the critical value for the bulk diffusion coefficient $D_{2,\mathrm{crit}}$ (which enters through $\eta$):

$$\frac{D_{2,\mathrm{crit}}}{D_1} = \left( \ln\left(\frac{2}{1-\cos\epsilon}\right) - \frac{1+\cos\epsilon}{2} \right) \frac{2(2aR - a^2)}{3R^2(\xi \cdot U)}$$

$$= \left( \ln\left(\frac{2}{1-\cos\epsilon}\right) - \frac{1+\cos\epsilon}{2} \right) \frac{2(1-x^2)}{3}$$

$$\times \left( \sum_{n=1}^{\infty} \frac{(1-x^n)(2n+1)}{n^2(n+1)^4} \left[ (n+1+n\cos\epsilon) P_n(\cos\epsilon) + P_{n-1}(\cos\epsilon) \right]^2 \right)^{-1}. \quad (80)$$

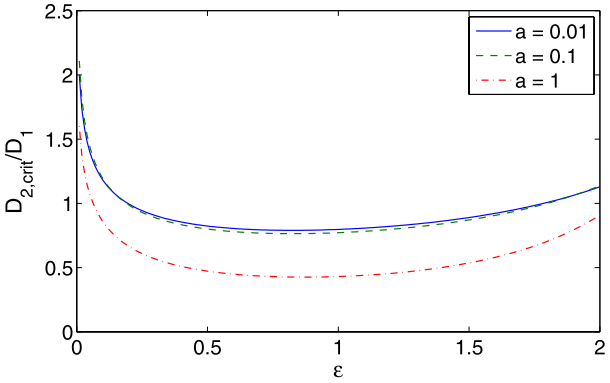


**Fig. 9** $D_{2,\mathrm{crit}}$ as a function of $\epsilon$ is computed from (80) in 3D for three values of $a/R$: 0.01, 0.1, and 1. When $\epsilon$ approaches $\pi$ (the whole surface becomes absorbing), $D_{2,\mathrm{crit}}$ diverges (not shown). In fact, in this limit, there is no need for a bulk excursion because the target will be found immediately by the surface diffusion. In addition, $D_{2,\mathrm{crit}}$ also diverges as $\epsilon \to 0$ because a point-like target cannot be detected neither by bulk excursions, nor by surface diffusion in 3D

In the limit of $\epsilon \to 0$, one gets

$$\frac{D_{2,\mathrm{crit}}}{D_1} \approx \frac{(2\ln(2/\epsilon)-1)(1-x^2)}{6}\left(\sum_{n=1}^{\infty}\frac{(1-x^n)(2n+1)}{n^2(n+1)^2}\right)^{-1} + O(\epsilon). \tag{81}$$

In the physically relevant limit $a \ll R$, one has

$$\frac{D_{2,\mathrm{crit}}}{D_1} \approx \frac{(2\ln(2/\epsilon)-1)}{3}\left(\sum_{n=1}^{\infty}\frac{2n+1}{n(n+1)^2}\right)^{-1} + O(\epsilon) = \frac{2(2\ln(2/\epsilon)-1)}{\pi^2} + O(\epsilon). \tag{82}$$

There are similarities and differences between the behaviors of $D_{2,\mathrm{crit}}$ in 2D and 3D. Figure 9 shows that $D_{2,\mathrm{crit}}$ from (82) is not a monotonous function of $\epsilon$, with the qualitative explanation which is the same as in the two-dimensional case.

In contrast to the analogous (39) in 2D, the r.h.s. of (82) diverges as $\epsilon \to 0$. This divergence reflects the fact that a point-like target ($\epsilon = 0$), which could be found within a finite time in 2D by one-dimensional surface diffusion on the circle, is not detectable in 3D neither by bulk excursions, nor by surface diffusion.

#### *4.6.2 When is there an Optimal Value of the Desorption Rate λ Minimizing the Search Time?*

For the reaction time to be an optimizable function of the desorption rate $\lambda$, it is necessary to write an additional condition, requiring that the bulk excursions are not "too favorable" (otherwise, the best strategy is obtained for $\lambda \to \infty$). A sufficient condition is given by demanding that the search time at zero desorption rate (i.e., without leaving the boundary) is less than the search time at infinite desorption rate

$$\langle t_1(\lambda = 0)\rangle < \langle t_1(\lambda \to \infty)\rangle, \tag{83}$$

$$\langle t_1(\lambda = 0)\rangle = \frac{R^2}{D_1}(2\ln(2/\epsilon) - 1) + O(\epsilon), \tag{84}$$

which writes in the physically relevant limit $a \ll R$ (using the result of [43]):

$$\langle t_1(\lambda \to \infty)\rangle = \frac{\pi R^2}{3\epsilon D_2}\left(1 + \epsilon\ln(1/\epsilon)\right). \tag{85}$$

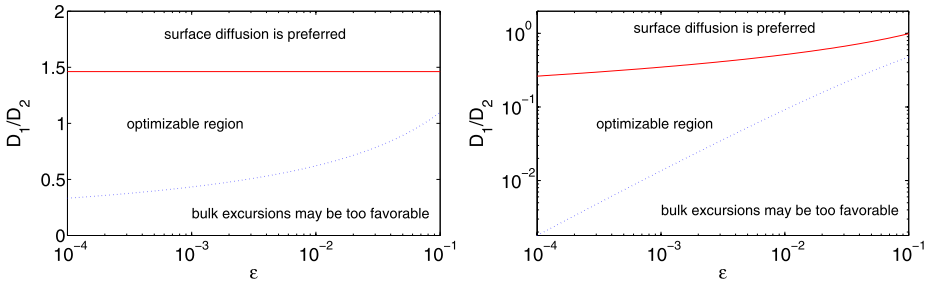


**Fig. 10** (Color online) The regions of optimality for the search time in 2D (*left*) and 3D (*right*). The lower bound (*solid blue line*) and upper bound (*dashed red line*) are given in the limit of $a \ll R$ and $\epsilon \ll 1$ by (43), (87) in 2D and 3D, respectively. When the ratio $D_1/D_2$ lies between two curves, the search time $\langle t_1 \rangle$ is optimizable with respect to $\lambda$. Above the upper bound, surface diffusion is preferred ($\lambda = 0$ is the optimal solution), while below the lower bound, bulk excursions may be "too favorable" ($\lambda \to \infty$ may give the optimal solution). We recall that the lower bound was obtained from the sufficient condition (83) meaning that the region below the dotted line may still be optimizable.

Finally, this conditions leads, for small $\epsilon$, to

$$\frac{D_1}{D_2} > \frac{3\epsilon}{\pi}(2\ln(2/\epsilon) - 1). \tag{86}$$

Combining the two conditions (82), (86), the search time is found to be optimizable when $a \ll R$ and $\epsilon \ll 1$ if

$$\frac{3\epsilon}{\pi}(2\ln(2/\epsilon) - 1) < \frac{D_1}{D_2} < \frac{\pi^2}{2(2\ln(2/\epsilon) - 1)}. \tag{87}$$

## 5 Numerical Resolution

In the previous sections, we derived the closed matrix forms (25), (65) for the coefficients $d_n$ in 2D and 3D. These coefficients determine the angular dependence of $t_1(\theta)$ through the explicit representations (20), (60) in 2D and 3D, respectively. Although the formulas (25), (65) which are based on the inversion of an infinite-dimensional matrix $(I - \Omega Q)$ remain implicit, a numerical resolution of the problem has become straightforward. In fact, one needs to truncate the infinite-dimensional matrix $Q$ and vectors $U$ and $\tilde{U}$ and to invert the truncated matrix $(I - \Omega Q)$ numerically.

There are six parameters that determine the function $t_1(\theta)$: the radius $R$ of the disk (sphere), the diffusion coefficients $D_1$ and $D_2$, the desorption rate $\lambda$, the size $\epsilon$ of the absorbing region, and the distance $a$. From now on, we set the units of length and time by setting $R = 1$ and $D_1 = 1$. Although the distance $a$ may take any value from 0 to $R$, the physically interesting case corresponds to the limit of small $a$. As we mentioned previously, the limit $a = 0$ exists but trivially leads to searching on the surface, without intermediate bulk excursions. In order to reveal the role of $a$, we consider several values of $a$: 0.001, 0.01, 0.1 and 1, the latter corresponding to the specific situation when search is always restarted from the center. Since the diffusion coefficient $D_2$ enters only through the prefactor $T$ from (10), its influence onto the searching time $t_1$ is easy to examine. In what follows, we take three

values of $D_2$: 0.1, 1 and 10. The dependence of $t_1$ on the desorption rate $\lambda$ and the size $\epsilon$ is the most interesting issue which will be studied below.

In the previous sections, we derived several formulas for computing $t_1$:

- explicit representations (20), (60) with the exact expressions (25), (65) for the coefficients;
- approximations (32), (75) which were derived by neglecting non-diagonal elements of the matrix $Q$;
- perturbative formulas (11), (71) which are valid for small $\epsilon$.

For a numerical computation of the coefficients in (25), (65), we truncate the infinite-dimensional matrix $Q$ to a finite size $N \times N$ and invert the matrix $(I - \Omega Q)$. In order to check the accuracy of this scheme, we compute the coefficients by taking several values of $N$ from 10 to 200. For $D_2 = 1$, $\epsilon = 0.1$, $a = 0.01$ and $\lambda = 1$, the computed mean time $\langle t_1 \rangle$ rapidly converges to a limit. Even the computation with $N = 10$ gives the result with four significant digits. Note that other sets of parameters (e.g., larger values of $\Omega$) may require larger truncation sizes.

## 6 Conclusion

To conclude, we have presented an exact calculation of the mean first-passage time to a target on the surface of a 2D and 3D spherical domain, for a molecule performing surface-mediated diffusion. The presented approach is based on an integral equation which can be solved analytically, and numerically validated approximation schemes, which provide more tractable expressions of the mean FPT. This minimal model of surface-mediated reactions, which explicitly takes into account the combination of surface and bulk diffusions, shows the importance of correlations induced by the coupling of the switching dynamics to the geometry of the confinement. Indeed, standard MF treatments prove to substantially underestimate the reaction time in this case [6], and sometimes even fail to reproduce the proper monotonicity [39]. In the context of interfacial systems in confinement, our results show that the reaction time can be minimized as a function of the desorption rate from the surface, which puts forward a general mechanism of enhancement and regulation of chemical reactivity.

## Appendix A: Another Approach in 2D

In this appendix, we describe another theoretical approach which relies on the explicit form of the Green function of the Poisson equation in 2D case. In particular, the perturbative analysis for small $\epsilon$ becomes easier within this approach.

Considering $t_2$ as a source term in the Poisson type equation (1) with absorbing conditions at $\theta = \epsilon$ and $\theta = 2\pi - \epsilon$ whose Green function is well known [44], $t_1$ writes

$$t_1(\theta) = \frac{1}{\omega \sinh(2\omega(\pi - \epsilon))} \int_{\epsilon}^{2\pi-\epsilon} \sinh(\omega(\theta_< - \epsilon)) \sinh(\omega(2\pi - \epsilon - \theta_>)) \times \left[ \frac{R^2}{D_1} + \frac{\lambda R^2}{D_1} t_2(R - a, \theta') \right] \mathrm{d}\theta', \tag{A.1}$$

and the notations $\theta_< = \min(\theta, \theta')$ and $\theta_> = \max(\theta, \theta')$.

Injecting (5) into (A.1) leads to

$$t_1(\theta) = \frac{\omega}{\lambda \sinh(2\omega(\pi-\epsilon))}\left(\mathrm{I}(0,\theta)\left(1+\lambda\left(\alpha_0 - \frac{(R-a)^2}{4D_2}\right)\right) + \lambda\sum_{m=1}^{\infty}\alpha_m (R-a)^m \mathrm{I}(m,\theta)\right), \tag{A.2}$$

where, for $m$ integer,

$$\begin{aligned}\mathrm{I}(m,\theta) &\equiv \int_{\epsilon}^{2\pi-\epsilon} \sinh(\omega(\theta_< - \epsilon))\sinh(\omega(2\pi-\epsilon-\theta_>))\cos(m\theta')\,\mathrm{d}\theta' \\ &= \frac{\omega}{\omega^2+m^2}(\cos(m\theta)\sinh(2\omega(\pi-\epsilon)) \\ &\quad - 2\cos(m\epsilon)\sinh(\omega(\pi-\epsilon))\cosh(\omega(\theta-\pi))),\end{aligned} \tag{A.3}$$

so that

$$\begin{aligned}t_1(\theta) &= \frac{1}{\lambda} + \alpha_0 - \frac{(R-a)^2}{4D_2} + \omega^2\sum_{m=1}^{\infty}\frac{\alpha_m}{\omega^2+m^2}(R-a)^m\cos(m\theta) \\ &\quad - \frac{\cosh(\omega(\theta-\pi))}{\cosh(\omega(\pi-\epsilon))}\left(\frac{1}{\lambda} + \alpha_0 - \frac{(R-a)^2}{4D_2}\right. \\ &\quad \left. + \omega^2\sum_{m=1}^{\infty}\frac{\alpha_m}{\omega^2+m^2}(R-a)^m\cos(m\epsilon)\right).\end{aligned} \tag{A.4}$$

Substituting (A.4) into (7) gives

$$\begin{aligned}S\frac{\tanh(\omega(\pi-\epsilon))}{\omega\pi} &= -\frac{\epsilon}{\pi}\lambda\alpha_0 + 1 - \frac{\epsilon}{\pi} + \lambda\left(\frac{R^2}{4D_2} - \left(1-\frac{\epsilon}{\pi}\right)\frac{(R-a)^2}{4D_2}\right) \\ &\quad - \frac{\lambda\omega^2}{\pi}\sum_{m=1}^{\infty}\frac{\alpha_m}{\omega^2+m^2}(R-a)^m\frac{\sin(m\epsilon)}{m},\end{aligned} \tag{A.5}$$

and

$$\begin{aligned}&\lambda\left(R^n - \frac{\omega^2}{\omega^2+n^2}\left(1-\frac{\epsilon}{\pi}\right)(R-a)^n\right)\alpha_n \\ &= -\frac{2\sin(n\epsilon)}{n\pi}\left(1+\lambda\left(\alpha_0 - \frac{(R-a)^2}{4D_2}\right)\right) \\ &\quad - \frac{\lambda\omega^2}{\pi}\left(\sum_{m\neq n}\frac{\alpha_m}{\omega^2+m^2}(R-a)^m\frac{\sin((m-n)\epsilon)}{m-n}\right. \\ &\quad \left. + \sum_{m=1}^{\infty}\frac{\alpha_m}{\omega^2+m^2}(R-a)^m\frac{\sin((m+n)\epsilon)}{m+n}\right) \\ &\quad - \frac{2\tanh(\omega(\pi-\epsilon))}{\pi(\omega^2+n^2)}S\left(\omega\cos(n\epsilon) - \frac{n\sin(n\epsilon)}{\tanh(\omega(\pi-\epsilon))}\right),\end{aligned} \tag{A.6}$$

where

$$S \equiv 1 + \lambda \left( \alpha_0 - \frac{(R-a)^2}{4D_2} \right) + \lambda\omega^2 \sum_{m=1}^{\infty} \frac{\alpha_m}{\omega^2 + m^2} (R-a)^m \cos(m\epsilon). \tag{A.7}$$

Equation (A.5) can be rearranged into

$$\begin{aligned} &\left( \alpha_0 - \frac{R^2}{4D_2} \right) \left( \frac{\epsilon}{\pi} + \frac{\tanh(\omega(\pi-\epsilon))}{\pi\omega} \right) \\ &\quad = \left( \frac{1}{\lambda} + \left( \frac{R^2}{4D_2} - \frac{(R-a)^2}{4D_2} \right) \right) \left( 1 - \frac{\epsilon}{\pi} - \frac{\tanh(\omega(\pi-\epsilon))}{\pi\omega} \right) \\ &\qquad - \frac{\omega}{\pi} \sum_{n=1}^{\infty} \frac{(R-a)^n}{\omega^2 + n^2} \left( \tanh(\omega(\pi-\epsilon)) \cos(n\epsilon) + \frac{\omega}{n} \sin(n\epsilon) \right) \alpha_n, \end{aligned} \tag{A.8}$$

and (A.6) into

$$\begin{aligned} &\left( R^n - \frac{\omega^2}{\omega^2 + n^2} \left( 1 - \frac{\epsilon}{\pi} \right) (R-a)^n \right) \alpha_n \\ &\quad = -\frac{2}{\pi n} \left( \alpha_0 - \frac{R^2}{4D_2} + T \right) \left( \frac{\omega^2}{\omega^2 + n^2} \sin(n\epsilon) + \frac{n\omega}{\omega^2 + n^2} \tanh(\omega(\pi-\epsilon)) \cos(n\epsilon) \right) \\ &\qquad - \frac{2\omega^2}{\pi(\omega^2 + n^2)} \sum_{m=1}^{\infty} \alpha_m \frac{(R-a)^m}{\omega^2 + m^2} \cos(m\epsilon) (\omega \cos(n\epsilon) \tanh(\omega(\pi-\epsilon)) - n \sin(n\epsilon)) \\ &\qquad - \frac{\omega^2}{\pi} \left( \sum_{m \neq n} \frac{\alpha_m}{\omega^2 + m^2} (R-a)^m \frac{\sin((m-n)\epsilon)}{m-n} \right. \\ &\qquad \left. + \sum_{m=1}^{\infty} \frac{\alpha_m}{\omega^2 + m^2} (R-a)^m \frac{\sin((m+n)\epsilon)}{m+n} \right). \end{aligned} \tag{A.9}$$

### A.1 Particular Case $\lambda = 0$

In this case, the previous equations can be solved exactly, leading to

$$\alpha_0 - \frac{R^2}{4D_2} = \frac{1}{3} \frac{R^2}{D_1} \frac{(\pi-\epsilon)^3}{\pi}, \tag{A.10}$$

and

$$\alpha_n = -\frac{2}{\pi} \frac{R^2}{D_1} \frac{n(\pi-\epsilon)\cos(n\epsilon) + \sin(n\epsilon)}{n^3} \frac{1}{R^n}. \tag{A.11}$$

We note that the particular case $a = 0$ is also described by these expressions, although it does not seem to be clear from (A.5)–(A.6).

### A.2 Particular Case $a = R$

Here again, (A.5)–(A.6) can be solved exactly, and give :

$$\alpha_0 - \frac{R^2}{4D_2} = \left( \frac{1}{\lambda} + \frac{R^2}{4D_2} \right) \frac{1 - \frac{\epsilon}{\pi} - \frac{\tanh(\omega(\pi-\epsilon))}{\pi\omega}}{\frac{\epsilon}{\pi} + \frac{\tanh(\omega(\pi-\epsilon))}{\pi\omega}}, \tag{A.12}$$

and

$$\alpha_n = -\frac{2}{\pi}\left(\frac{1}{\lambda}+\frac{R^2}{4D_2}\right)\frac{\omega}{\omega^2+n^2}\frac{\frac{\omega}{n}\sin(n\epsilon)+\tanh(\omega(\pi-\epsilon))\cos(n\epsilon)}{\frac{\epsilon}{\pi}+\frac{\tanh(\omega(\pi-\epsilon))}{\pi\omega}}\frac{1}{R^n}. \tag{A.13}$$

### A.3 Perturbative Approach

Expanding $\alpha_0$ and $\alpha_n$ in powers of $\epsilon$

$$\alpha_0 = \alpha_0^{(0)}+\alpha_0^{(1)}\epsilon+\alpha_0^{(2)}\epsilon^2+\cdots \quad \text{and} \quad \alpha_n = \alpha_n^{(0)}+\alpha_n^{(1)}\epsilon+\alpha_n^{(2)}\epsilon^2+\cdots \tag{A.14}$$

Equations (A.5)–(A.6) lead, after lengthy calculations, to

$$\begin{aligned}\alpha_0 &= \frac{R^2}{4D_2}+\omega^2 T\left\{\left(2\sum_{m=1}^{\infty}\frac{1}{\omega^2(1-x^m)+m^2}\right)\right.\\ &\left.-\pi\epsilon+\left(1+2\omega^2\sum_{m=1}^{\infty}\frac{1-x^m}{\omega^2(1-x^m)+m^2}\right)\epsilon^2\right\}+\cdots,\\ \alpha_n &= \frac{\omega^2 T}{R^n(\omega^2(1-x^n)+n^2)}\left\{-2+n^2\epsilon^2+\cdots\right\}.\end{aligned} \tag{A.15}$$

## Appendix B: A second Integral Equation Satisfied by $t_1$ in the 2D Case

Using (7) for the Fourier coefficients in (A.4) leads to a second integral equation satisfied by $t_1$

$$\begin{aligned}t_1(\theta) &= T\left(1-\frac{\cosh(\omega(\pi-\theta))}{\cosh(\omega(\pi-\epsilon))}\right)\\ &+\int_{\epsilon}^{2\pi-\epsilon}t_1(\alpha)\left(J(\theta,\alpha)-\frac{\cosh(\omega(\pi-\theta))}{\cosh(\omega(\pi-\epsilon))}J(\epsilon,\alpha)\right)\mathrm{d}\alpha,\end{aligned} \tag{B.1}$$

where

$$J(\theta,\alpha)\equiv\frac{1}{2\pi}+\frac{1}{\pi}\sum_{n=1}^{\infty}\frac{\omega^2}{\omega^2+n^2}\left(1-\frac{a}{R}\right)^n\cos(n\theta)\cos(n\alpha). \tag{B.2}$$

This equation is especially well adapted to local expansions of $t_1(\theta)$ in the vicinity of $a\simeq R$, but it can also be rearranged into the following integral equation, useful when $a\ll R$ :

$$\begin{aligned}t_1(\theta) &= T\left(1-\frac{\cosh(\omega(\pi-\theta))}{\cosh(\omega(\pi-\epsilon))}\right)+\frac{\omega}{\sinh(2\omega(\pi-\epsilon))}\\ &\times\int_{\epsilon}^{2\pi-\epsilon}t_1(\theta')\sinh(\omega(\theta_<-\epsilon))\sinh(\omega(2\pi-\epsilon-\theta_>))\,\mathrm{d}\theta'\\ &+\int_{\epsilon}^{2\pi-\epsilon}t_1(\alpha)\left(\widetilde{J}(\theta,\alpha)-\frac{\cosh(\omega(\pi-\theta))}{\cosh(\omega(\pi-\epsilon))}\widetilde{J}(\epsilon,\alpha)\right)\mathrm{d}\alpha,\end{aligned} \tag{B.3}$$

where

$$\widetilde{J}(\theta,\alpha) \equiv \frac{1}{\pi}\sum_{n=1}^{\infty}\frac{\omega^2}{\omega^2+n^2}\left(\left(1-\frac{a}{R}\right)^n-1\right)\cos(n\theta)\cos(n\alpha). \tag{B.4}$$

## Appendix C: Computation of $I_\epsilon(m,n)$ in 3D

In this appendix, we provide the explicit formula for the matrix $I_\epsilon(m,n)$ in 3D case. Although technical, this is an important result for a numerical computation because it allows one to avoid an approximate integration in (64) which otherwise could be a significant source of numerical errors. The formula (C.6) for non-diagonal elements is somewhat elementary, while the derivation for diagonal elements seems to be original.

### C.1 Non-Diagonal Elements

The Legendre polynomials satisfy

$$\frac{d}{dx}\left[(1-x^2)\frac{d}{dx}P_n(x)\right]+n(n+1)P_n(x)=0, \tag{C.1}$$

from which

$$\int_a^b dx\,P_n(x) = -\frac{[(1-x^2)P_n'(x)]_a^b}{n(n+1)} \quad (n>0) \tag{C.2}$$

and

$$\int_a^b dx\,P_m(x)P_n(x) = \frac{[(1-x^2)[P_m(x)P_n'(x)-P_n(x)P_m'(x)]]_a^b}{m(m+1)-n(n+1)} \quad (m\neq n). \tag{C.3}$$

Since

$$(1-x^2)P_n'(x) = -nxP_n(x)+nP_{n-1}(x) = (n+1)xP_n(x)-(n+1)P_{n+1}(x), \tag{C.4}$$

we find

$$\int_a^b dx\,P_n(x) = \frac{[xP_n(x)-P_{n-1}(x)]_a^b}{n+1} \quad (n>0) \tag{C.5}$$

and

$$\int_a^b dx\;P_m(x)P_n(x) = \frac{[(m-n)xP_m(x)P_n(x)+nP_{n-1}(x)P_m(x)-mP_{m-1}(x)P_n(x)]]_a^b}{m(m+1)-n(n+1)}$$
$$(m\neq n). \tag{C.6}$$

From the above formulas, we get

$$I_\epsilon(m,n) = m\frac{(n-m)uP_m(u)P_n(u)+(m+1)P_m(u)P_{n-1}(u)-(n+1)P_n(u)P_{m-1}(u)}{(n+1)[m(m+1)-n(n+1)]},$$
$$u=\cos\epsilon \quad (m\neq n). \tag{C.7}$$

C.2 Diagonal Elements

We denote

$$K_n = \int_a^b dx\, P_n^2(x). \tag{C.8}$$

Using the relation

$$P_n(x) = \frac{2n-1}{n} x P_{n-1}(x) - \frac{n-1}{n} P_{n-2}(x), \tag{C.9}$$

we obtain

$$K_n = \frac{2n-1}{n} \int_a^b dx\, x P_{n-1}(x) P_n(x) - \frac{n-1}{n} \int_a^b dx\, P_{n-2}(x) P_n(x). \tag{C.10}$$

The second integral is given by (C.6). In order to compute the first one, we consider

$$\begin{aligned} 0 &= \int_a^b dx \left\{ x P_{n-1}(x) \left[ \frac{d}{dx} \left[ (1-x^2) \frac{d}{dx} P_n(x) \right] + n(n+1) P_n(x) \right] \right. \\ &\quad \left. - x P_n(x) \left[ \frac{d}{dx} \left[ (1-x^2) \frac{d}{dx} P_{n-1}(x) \right] + (n-1) n P_{n-1}(x) \right] \right\} \\ &= 2n \int_a^b dx x P_{n-1}(x) P_n(x) + \left[ x P_{n-1}(x)(1-x^2) P_n'(x) - x P_n(x)(1-x^2) P_{n-1}'(x) \right]_a^b \\ &\quad - \int_a^b dx (1-x^2) \left[ P_n'(x) P_{n-1}(x) - P_{n-1}'(x) P_n(x) \right]. \end{aligned} \tag{C.11}$$

The last integral can be written as

$$\begin{aligned} J &= \int_a^b dx (1-x^2) P_n^2(x) (P_{n-1}(x)/P_n(x))' = \left[ (1-x^2) P_{n-1}(x) P_n(x) \right]_a^b \\ &\quad - \int_a^b dx (P_{n-1}(x)/P_n(x)) \left[ -2x P_n^2(x) + 2(1-x^2) P_n'(x) P_n(x) \right] \\ &= \left[ (1-x^2) P_{n-1}(x) P_n(x) \right]_a^b - 2 \int_a^b dx \left[ -x P_{n-1}(x) P_n(x) + (1-x^2) P_n'(x) P_{n-1}(x) \right]. \end{aligned} \tag{C.12}$$

In the last term, we substitute $(1-x^2) P_n'(x)$ to get

$$\begin{aligned} J &= \left[ (1-x^2) P_{n-1}(x) P_n(x) \right]_a^b + 2 \int_a^b dx\, x P_{n-1}(x) P_n(x) \\ &\quad - 2 \int_a^b dx \left[ -nx P_n(x) + n P_{n-1}(x) \right] P_{n-1}(x). \end{aligned} \tag{C.13}$$

Bringing these results together, we get

$$0 = 2n \int_a^b dx\, x P_{n-1}(x) P_n(x) + \left[ x P_{n-1}(x)(1-x^2) P_n'(x) - x P_n(x)(1-x^2) P_{n-1}'(x) \right]_a^b$$

$$+\left[(1-x^2)P_{n-1}(x)P_n(x)\right]_a^b + 2\int_a^b dx\, x P_{n-1}(x)P_n(x)$$
$$-2\int_a^b dx\left[-nxP_n(x)+nP_{n-1}(x)\right]P_{n-1}(x) \tag{C.14}$$

so that

$$\int_a^b dx\, x P_{n-1}(x)P_n(x) = \frac{-1}{4n+2}\Big[x(1-x^2)\big[P_{n-1}(x)P_n'(x) - P_n(x)P_{n-1}'(x)\big] + (1-x^2)P_{n-1}(x)P_n(x)\Big]_a^b + \frac{n}{2n+1}K_{n-1}. \tag{C.15}$$

We obtain

$$K_n = -\frac{2n-1}{2n(2n+1)}\Big[x(1-x^2)\big[P_{n-1}(x)P_n'(x) - P_n(x)P_{n-1}'(x)\big] + (1-x^2)P_{n-1}(x)P_n(x)\Big]_a^b + \frac{2n-1}{2n+1}K_{n-1} - \frac{n-1}{n}\left[\frac{2xP_{n-2}(x)P_n(x) - nP_{n-1}(x)P_{n-2}(x) + (n-2)P_{n-3}(x)P_n(x)}{2(2n-1)}\right]_a^b. \tag{C.16}$$

We can further simplify this expression by using the following identities

$$\begin{aligned}(n-1)P_{n-1}(x) - (2n-3)xP_{n-2}(x) + (n-2)P_{n-3}(x) &= 0,\\ nP_n(x) - (2n-1)xP_{n-1}(x) + (n-1)P_{n-2}(x) &= 0,\\ (1-x^2)P_n'(x) &= -nxP_n(x) + nP_{n-1}(x),\\ (1-x^2)P_{n-1}'(x) &= nxP_{n-1}(x) - nP_n(x).\end{aligned} \tag{C.17}$$

We get

$$\begin{aligned}K_n &= -\frac{2n-1}{2n(2n+1)}\Big[nx\big[P_{n-1}^2(x) + P_n^2(x) - 2xP_n(x)P_{n-1}(x)\big] + (1-x^2)P_{n-1}(x)P_n(x)\Big]_a^b + \frac{2n-1}{2n+1}K_{n-1} - \frac{n-1}{2n(2n-1)}\\ &\quad\times\left[(2n-1)xP_n(x)P_{n-2}(x) - nP_{n-1}(x)P_{n-2}(x) - (n-1)P_{n-1}(x)P_n(x)\right]_a^b\\ &= -\frac{2n-1}{2n(2n+1)}\Big[nx\big[P_{n-1}^2(x) + P_n^2(x) - 2xP_n(x)P_{n-1}(x)\big] + (1-x^2)P_{n-1}(x)P_n(x)\Big]_a^b + \frac{2n-1}{2n+1}K_{n-1}\\ &\quad - \frac{1}{2n}\Big[((2n-1)x^2+1)P_n(x)P_{n-1}(x) - nx(P_{n-1}^2(x) + P_n^2(x))\Big]_a^b\\ &= \frac{[x(P_{n-1}^2(x) + P_n^2(x)) - 2P_n(x)P_{n-1}(x)]_a^b}{2n+1} + \frac{2n-1}{2n+1}K_{n-1}\end{aligned} \tag{C.18}$$

and we know that $K_0 = b - a$. Applying this formula recursively, one finds

$$K_n = \frac{F_n(b) - F_n(a)}{2n+1}, \tag{C.19}$$

where

$$\begin{aligned} F_n(x) &= x[P_n^2(x) + 2P_{n-1}^2(x) + \cdots + 2P_1^2(x) + P_0(x)] \\ &\quad - 2P_n(x)P_{n-1}(x) - 2P_{n-1}(x)P_{n-2}(x) - \cdots - 2P_1(x)P_0(x) + x \\ &= \sum_{k=1}^{n} \big[2(x-1)P_k^2(x) + [P_k(x) - P_{k-1}(x)]^2\big] - (x-1)P_n^2(x) + (x-1)P_0^2(x) + x. \end{aligned} \tag{C.20}$$

One can check that this function satisfies the recurrent relation

$$F_n(x) = F_{n-1}(x) + x[P_n^2(x) + P_{n-1}^2(x)] - 2P_n(x)P_{n-1}(x), \qquad F_0(x) = x. \tag{C.21}$$

Note that $F_n(\pm 1) = F_{n-1}(\pm 1) = \cdots = \pm 1$.

As a result, we obtain

$$I_\epsilon(n,n) = -P_n(u)\frac{uP_n(u) - P_{n-1}(u)}{n+1} + \frac{F_n(u)+1}{2n+1}, \quad u = \cos\epsilon. \tag{C.22}$$

## References


1. Rice, S.A.: Diffusion-Limited Reactions, vol. 25. Elsevier, Amsterdam (1985)
2. Hänggi, P., Talkner, P., Borkovec, M.: Rev. Mod. Phys. **62**, 251 (1990)
3. Alberts, B., Johnson, A., Lewis, J., Raff, M., Roberts, K., Walter, P.: Molecular Biology of the Cell. Garland, New York (2002)
4. Bénichou, O., et al.: Phys. Rev. Lett. **94**, 198101 (2005)
5. Bénichou, O., et al.: J. Phys., Condens. Matter **17**, S4275 (2005)
6. Bénichou, O., Loverdo, C., Moreau, M., Voituriez, R.: Phys. Chem. Chem. Phys. **10**, 7059 (2008)
7. Coppey, M., Bénichou, O., Voituriez, R., Moreau, M.: Biophys. J. **87**, 1640 (2004)
8. Berg, O.G., Winter, R.B., von Hippel, P.H.: Biochemistry **20**, 6929 (1981)
9. Slutsky, M., Mirny, L.A.: Biophys. J. **87**, 4021 (2004)
10. Eliazar, I., Koren, T., Klafter, J.: J. Phys. Condens. Matter **19**, 065140 (2007)
11. Lomholt, M.A., Ambjornsson, T., Metzler, R.: Phys. Rev. Lett. **95**, 260603 (2005)
12. Bénichou, O., Coppey, M., Moreau, M., Suet, P.H., Voituriez, R.: Europhys. Lett. **70**, 42 (2005)
13. Levitz, P., et al.: Phys. Rev. Lett. **96**, 180601 (2006)
14. Levitz, P., et al.: Phys. Rev. E **78**, 030102 (2008)
15. Chechkin, A.V., Zaid, I.M., Lomholt, M.A., Sokolov, I.M., Metzler, R.: Phys. Rev. E **79** (2009)
16. Loverdo, C., Bénichou, O., Voituriez, R., Biebricher, A., Bonnet, I., Desbiolles, P.: Phys. Rev. Lett. **102**, 188101 (2009)
17. Adam, G., Delbrück, M.: Reduction of Dimensionality in Biological Diffusion Processes. Freeman, San Francisco (1968)
18. Sano, H., Tachiya, M.: J. Chem. Phys. **75**, 2870 (1981)
19. Astumian, R.D., Chock, P.B.: J. Phys. Chem. **89**, 3477 (1985)
20. Bond, G.C.: Heterogeneous Catalysis: Principles and Applications. Clarendon, Oxford (1987)
21. Blumen, A., Zumofen, G., Klafter, J.: Physical Review B **30** (1984)
22. Schuss, Z., Singer, A., Holcman, D.: Proc. Natl. Acad. Sci. USA **104**, 16098 (2007)
23. Kozak, J.J., Balakrishnan, V.: Phys. Rev. E **65** (2002)
24. Condamin, S., et al.: Nature **450**, 77 (2007)

25. Bénichou, O., Meyer, B., Tejedor, V., Voituriez, R.: Phys. Rev. Lett. **101**, 130601 (2008)
26. Tejedor, V., Bénichou, O., Voituriez, R.: Phys. Rev. E **80**, 065104 (2009)
27. Agliari, E.: Phys. Rev. E, Stat. Nonlinear Soft Matter Phys. **77**, 011128 (2008)
28. Haynes, C.P., Roberts, A.P.: Phys. Rev. E, Stat. Nonlinear Soft Matter Phys. **78**, 041111 (2008)
29. Reuveni, S., Granek, R., Klafter, J.: Phys. Rev. E **81**, 040103 (2010)
30. Redner, S.: A Guide to First-Passage Processes. Cambridge University Press, Cambridge (2001)
31. Condamin, S., Bénichou, O., Moreau, M.: Phys. Rev. Lett. **95**, 260601 (2005)
32. Condamin, S., Bénichou, O., Moreau, M.: Phys. Rev. E **75**, 021111 (2007)
33. Grebenkov, D.S.: Phys. Rev. E, Stat. Nonlinear Soft Matter Phys. **76**, 041139 (2007)
34. Condamin, S., Bénichou, O., Klafter, J.: Phys. Rev. Lett. **98**, 250602 (2007)
35. Singer, A., Schuss, Z., Holcman, D.: J. Stat. Phys. **122**, 465 (2006)
36. Pillay, S., Ward, M.J., Peirce, A., Kolokolnikov, T.: Multiscale Model. Simul. **8**, 803 (2010)
37. Cheviakov, A.F., Ward, M.J., Straube, R.: Multiscale Model. Simul. **8**, 836 (2010)
38. Bénichou, O., Voituriez, R.: Phys. Rev. Lett. **100**, 168105 (2008)
39. Oshanin, G., Tamm, M., Vasilyev, O.: J. Chem. Phys. **132**, 235101 (2010)
40. Chevalier, C., Bénichou, O., Meyer, B., Voituriez, R.: J. Phys. A, Math. Theor. **44**, 025002 (2011)
41. Grigoriev, I.V., Makhnovskii, Y.A., Berezhkovskii, A.M., Zitserman, V.Y.: J. Chem. Phys. **116**, 9574 (2002)
42. Bénichou, O., Grebenkov, D., Levitz, P., Loverdo, C., Voituriez, R.: Phys. Rev. Lett. **105**, 150606 (2010)
43. Singer, A., Schuss, Z., Holcman, D., Eisenberg, R.: J. Stat. Phys. **122**, 437 (2006)
44. Barton, G.: Elements of Green's Functions and Propagation. Oxford Science Publications, Oxford (1989)